ANNUAL STATUS REPORT
Millimeter-Wavelengths Propagation Studies

The Ohio State University

ElectroScience Laboratory

(formerly Antenna Laboratory)
Department of Electrical Engineering
Columbus, Ohio 43212

ANNUAL STATUS REPORT 2374-2
1 November 1968

Grant Number NGR 36-008-080

National Aeronautics and Space Administration
Office of Grants and Research Contracts
Washington, D.C. 20546

NOTICES

When Government drawings, specifications, or other data are used for any purpose other than in connection with a definitely related Government procurement operation, the United States Government thereby incurs no responsibility nor any obligation whatsoever, and the fact that the Government may have formulated, furnished, or in any way supplied the said drawings, specifications, or other data, is not to be regarded by implication or otherwise as in any manner licensing the holder or any other person or corporation, or conveying any rights or permission to manufacture, use, or sell any patented invention that may in any way be related thereto.

The Government has the right to reproduce, use, and distribute this report for governmental purposes in accordance with the contract under which the report was produced. To protect the proprietary interests of the contractor and to avoid jeopardy of its obligations to the Government, the report may not be released for non-governmental use such as might constitute general publication without the express prior consent of The Ohio State University Research Foundation.

REPORT 2374-2

REPORT

by

The Ohio State University ElectroScience Laboratory
(Formerly Antenna Laboratory)
Columbus, Ohio 43212

Sponsor	National Aeronautics and Space Administration Office of Grants and Research Contracts Washington, D. C. 20546
Grant Number	NGR 36-008-080
Investigation of	Millimeter-Wavelengths Propagation Studies
Subject of Report	Annual Status Report
Submitted by	ElectroScience Laboratory Department of Electrical Engineering The Ohio State University
Date	1 November 1968
Investigators	Peter Bohley Robert L. Riegler

ABSTRACT

Preparations for Ohio State University participation in the NASA ATS-E millimeter wave experiment are described. Two terminals are under construction and will be used for space diversity experiments.

The results of a study to determine some of the effects of the atmosphere on earth/space communications links are presented.

CONTENTS

ANNUAL STATUS REPORT
1 September 1967 - 31 August 1968

INTRODUCTION

The use of microwaves for commercial communications purposes has increased greatly in the last decade. So much so that serious crowding is being experienced at commonly used centimeter wavelengths. The exploitation of the relatively little used millimeter wavelengths to relieve some of this crowding has been proposed. Unfortunately the atmosphere is lossy and somewhat dispersive at these wavelengths particularly during severe weather. The present Grant was, in part, directed toward an investigation of these atmospheric effects in light of the forthcoming ATS-E millimeter wave propagation experiment.

During the latter portion of this reporting period work was started on the preliminary design and partial construction of two 15.3 GHz receiving stations for use in the ATS-E experiment. These terminals will be used for propagation studies and will also test the effectiveness of space diversity during severe weather conditions.

THEORETICAL STUDIES

In order to better understand the effects of the atmosphere on communications at 16 GHz the initial work during this Grant period was confined to accumulating and interrelating relevant material from the literature. It was found that considerable information exists. A very good compilation can be found in Reference 1. However the application of this information is far from simple.

In clear weather it appears that only small variations in atmospheric propagation paths will be noticed at 16 GHz (see Appendix). Path loss is of the order of a few tenths to one dB and antenna noise temperature varies from a few degrees to over 100 degrees, both as a function of humidity and zenith angle.

As the moisture content in the atmosphere increases, in the form of rain, snow and ice, theoretical approaches to the determination of propagation path degradation must depend upon statistical models to represent a nonhomogeneous volume. This nonhomogeneous volume is, in cross section the antenna collecting aperture, and in length the distance from the aperture to the edge of the atmosphere. The atmosphere surrounding this volume must also be considered because its

scattering effect will redirect signal energy to the aperture that would normally not have been collected. These volumes are nonhomogeneous because of the wide variations of rainfall (or ice or snow) rates within the relatively large distances involved. Particle size variation is also important.

In order to verify theoretical models to the point where they may be useful it appears that experimental results must be obtained that provide a three dimensional picture of the atmosphere. Presently, it appears that the closest approach to this picture may be obtained by the simultaneous measurement of radar backscatter, antenna noise temperature and signal attenuation, all at a single antenna. A synchronous satellite facilitates such measurements and should be useful in providing additional statistics toward this end.

It is known that storm cells of high intensity, those most likely to produce high attenuation at millimeter wavelengths, are relatively small in physical size. Two or more interconnected terminals spaced at distances that would prevent severe fading at all sites simultaneously would have certain benefits. The dynamic range requirements of the multiple terminal system could be considerably reduced over the single terminal system. This would mean smaller antennas and lower power transmitters could be used. This concept, termed space diversity, can be evaluated by the use of a synchronous satellite and two ground stations. Data would be recorded for various separation distances between sites. This data along with radar PPI photographs of the storm cells, encountered, should provide some insight into optimum spacing between sites. The experiment would also provide information on attendant problems such as the optimum method for combining the signals from each terminal, and the level of sophistication required at each terminal. The results of such an experiment would have considerable influence in the design of millimeter communications with satellites.

PREPARATION FOR THE EXPERIMENT

Plans for the preparation of two 15.3 GHz receiving stations have been completed. The south reflector of the Ohio State University Satellite Communications Facility four antenna array will be modified to accept the NASA phase locked receiver RF head and sufficient space provided in the control building for recording and control equipment. The antenna is configured for Cassegrainian feed and the existing sub reflector will be used. It is planned to illuminate less than the full 30 foot diameter of the parabolic reflector. The tolerance of the outer

panels of this surface is not sufficient to realize full gain at 15 GHz.

The second, moveable, terminal is under construction. An 18 × 8 foot flat bed trailer has been purchased and modified with four four-foot outrigger support points for increased stability. The antenna mount has been overhauled and new azimuth and elevation drive motors and synchos added. The mount will be fostered to the trailer, over the axle, by a 48 inch high tub spacer. The 15 foot parabolic reflector ordered during this period has been received. It has an F/D ratio of 0.4 and a surface tolerance of plus or minus 0.050 inches maximum in winds up to 30 miles per hour. An 18 inch central cutout will facilitate the use of a silo for the Cassegrainian feed planned. The antenna will be fastened to the antenna mount by a 19 inch spacer.

The feed package for both antennas will contain a phase locked receiver RF head, a 15 GHz radiometer and a calibrated noise sourse for calibration checks on both systems. A polarization splitter will be used to couple the two receivers to the antenna with no appreciable change in signal-to-noise ratio to either. This device will also decouple the receivers to some extent but to insure complete decoupling the radiometer center frequency will be shifted to one side of the 15.3 GHz channel.

The feed polarization of the moveable terminal antenna will be remotely rotatable so that the exact polarity of the incoming signal can be determined. The feed horn of the fixed site will be adjusted once this determination has been made.

A beacon package is planned that will provide a source for boresighting and antenna patterns for both sites. The beacon will be located at the top of a 500 feet commercial television tower and can be seen at all proposed locations of the moveable terminal.

Presently it is planned to provide weather information only from the fixed terminal. Wind direction, wind velocity, temperature, relative humidity, and rain fall rate at one or two locations under the propagation path will be recorded. When the two terminals are close together this information may be recorded at both sites. Later, with greater separation between sites it may be desirable to measure these parameters at both sites.

In so far as possible the terminals will be operated simultaneously, initially at a separation of the order of 1000 feet. Subsequent sites for the moveable terminal of approximately 5 and 15 miles from the fixed terminal are available. Intermediate sites may be found if required.

It is expected that both terminals will be substantially complete with the exception of the phase locked receivers by January 1968. Delivery of the receivers by this date should allow time for the completion of the terminals by the anticipated May launch date of the ATS-E satellite.

CONCLUSIONS

The use of millimeter wavelengths, between the water vapor and oxygen resonance bands, will prove to be a useful addition to the crowded microwave spectrum below 12 GHz. Statistical data resulting from the forthcoming ATS-E millimeter wave experiment will produce a high level of confidence in the suitability of millimeter waves for commercial use.

The space diversity experiment utilizing the ATS-E satellite will provide statistical data that should point toward optimization of millimeter wave earth/space communications links. The use of 2 or more properly separated, interrelated ground terminals will considerably reduce the severe fading conditions that can exist at a single terminal during rain storms.

APPENDIX A

1. Introduction

The purpose of this Appendix is to review the effect of atmospheric turbulence on the propagation of electromagnetic waves in the microwave and mm wave region.

A brief theoretical review is given for the magnitude of amplitude and phase fluctuations as well as their spatial and frequency correlation properties. Existing experimental data are presented when possible to support the theory.

This theory is applied to the proposed 16 GHz propagation experiment in order to determine what types of results might be expected. The results show that in clear weather the fluctuations, both in amplitude and phase, would be small and well correlated both in frequency and space, and that the limiting factor for a communication link will be due to attenuation during rainstorms.

2. Absolute Phase Fluctuations

It is well known that the effect of a turbulent propagation medium, such as the atmosphere, is to cause the instantaneous phase of a received signal to fluctuate about its average value. In the microwave region the RMS value of these fluctuations can be calculated from a geometrical optics solution.

Consider a single ray propagating in the medium as shown in Fig. 1; the ray will not traverse a straight line but will be refracted about its average path due to the variations in dielectric constant along the path. As the ray propagates along the non-homogeneous path it suffers a series of phase delays. Since the increased length of the path is second order compared to the fluctuations in dielectric constant, the phase delay $d\phi$ suffered by a ray in traversing between ℓ and $\ell + d\ell$ is given by

$$d\phi = \beta(\ell)\, d\ell$$

where $\beta(\ell) = \omega\sqrt{\mu\epsilon} = \omega\sqrt{\mu_o\epsilon_o}\sqrt{\epsilon_r}$

letting $\sqrt{\epsilon_r} = \eta$, the refractive index and $k_o = \omega\sqrt{\mu_o\epsilon_o}$, the free space propagation constant then

$$d\phi = k_o \eta\, d\ell \ .$$

Let the index of refraction be described as

$$\eta = \bar{\eta} + \Delta\eta$$
$$\approx 1 + \Delta\eta$$

where $\bar{\eta}$ = mean value of η
$\Delta\eta$ = fluctuation about the mean

so that $d\phi = k_o(1 + \Delta\eta)d\ell$, which consists of a constant plus a fluctuating component of phase. The constant term represents a time delay due to the finite propagation velocity; the fluctuating component is due to variations in the atmosphere's permittivity.

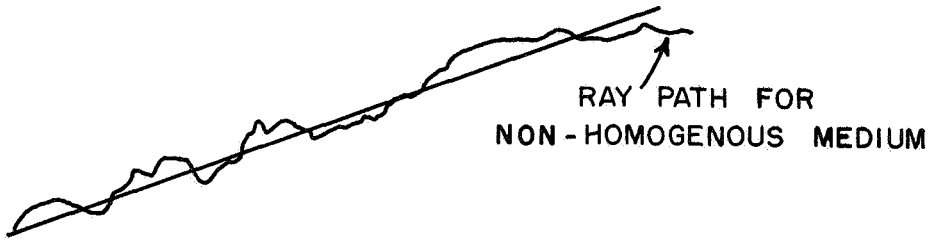

Fig. 1. Propagation path in the atmosphere.

The total phase fluctuation along a path of length L is then

$$\phi = \frac{2\pi}{\lambda} \int_0^L \Delta\eta(\ell)\, d\ell$$

Since the mean value of $\Delta\eta$ was defined to be zero ($\overline{\Delta\eta} = 0$) the average or mean value of ϕ will also be zero. The mean squared value $\overline{\phi^2}$ is

$$\overline{\phi^2} = \left(\frac{2\pi}{\lambda}\right)^2 \int_0^L \int_0^L \overline{\Delta\eta(\ell_1)\, \Delta\eta(\ell_2)}\, d\ell_1\, d\ell_2$$

In order to evaluate the integral an expression is required for the spatial correlation coefficient of refractive index $C_{\eta\eta}$ which is defined to be

$$C_{\eta\eta} = \frac{\overline{\Delta\eta(\ell_1)\, \Delta\eta(\ell_2)}}{\overline{\Delta\eta_2}}$$

where the overbar denotes ensemble average.

For isotropic turbulence the correlation coefficient is a function only of the magnitude of the distance between two points, i.e., $C_{\eta\eta}=C_{\eta\eta}(|\ell_1-\ell_2|)$.

Many models have been investigated for $C_{\eta\eta}$ and the corresponding RMS phase fluctuations calculated.[2] Among these are the following:

TABLE I

Model	$C_{\eta\eta}$	ϕ_{RMS}
Exponential	$\epsilon^{\frac{-\lvert r\rvert}{\ell_o}}$	$\frac{\sqrt{8\pi\sqrt{\ell_o L}}\,\Delta N\cdot 10^{-6}}{\lambda}$
Gaussian	$\epsilon^{\frac{-\lvert r\rvert^2}{\ell_o^2}}$	$\frac{\pi^{5/4}\sqrt{\ell_o L}\,\Delta N\cdot 10^{-6}}{\lambda}$
Cauchy	$\frac{1}{\left[1+\frac{\lvert r\rvert^2}{\ell_o^2}\right]^2}$	$\frac{\pi^{3/2}\sqrt{\ell_o L}\,\Delta N\cdot 10^{-6}}{\lambda}$

where

ℓ_o = characteristic scale of turbulence

ΔN = standard N unit representation $N = (\eta-1)\cdot 10^6$

$r = \ell_1 - \ell_2$.

It is interesting to note that the RMS value of phase fluctuations for the three correlation models are within a factor of two of each other; this indicated that $\overline{\phi^2}$ is relatively insensitive to the form of the correlation function and depends primarily on the value of the turbulence scale, ℓ_o.

The linear relationship between phase and frequency predicted by the geometrical optics solution is experimentally verified quite well by Fig. 2, which shows a simultaneous measurement of phase made over almost a 100:1 range of frequencies. The theoretical predictions based on the exponential correlation model for average meteorological conditions is also shown for comparison.

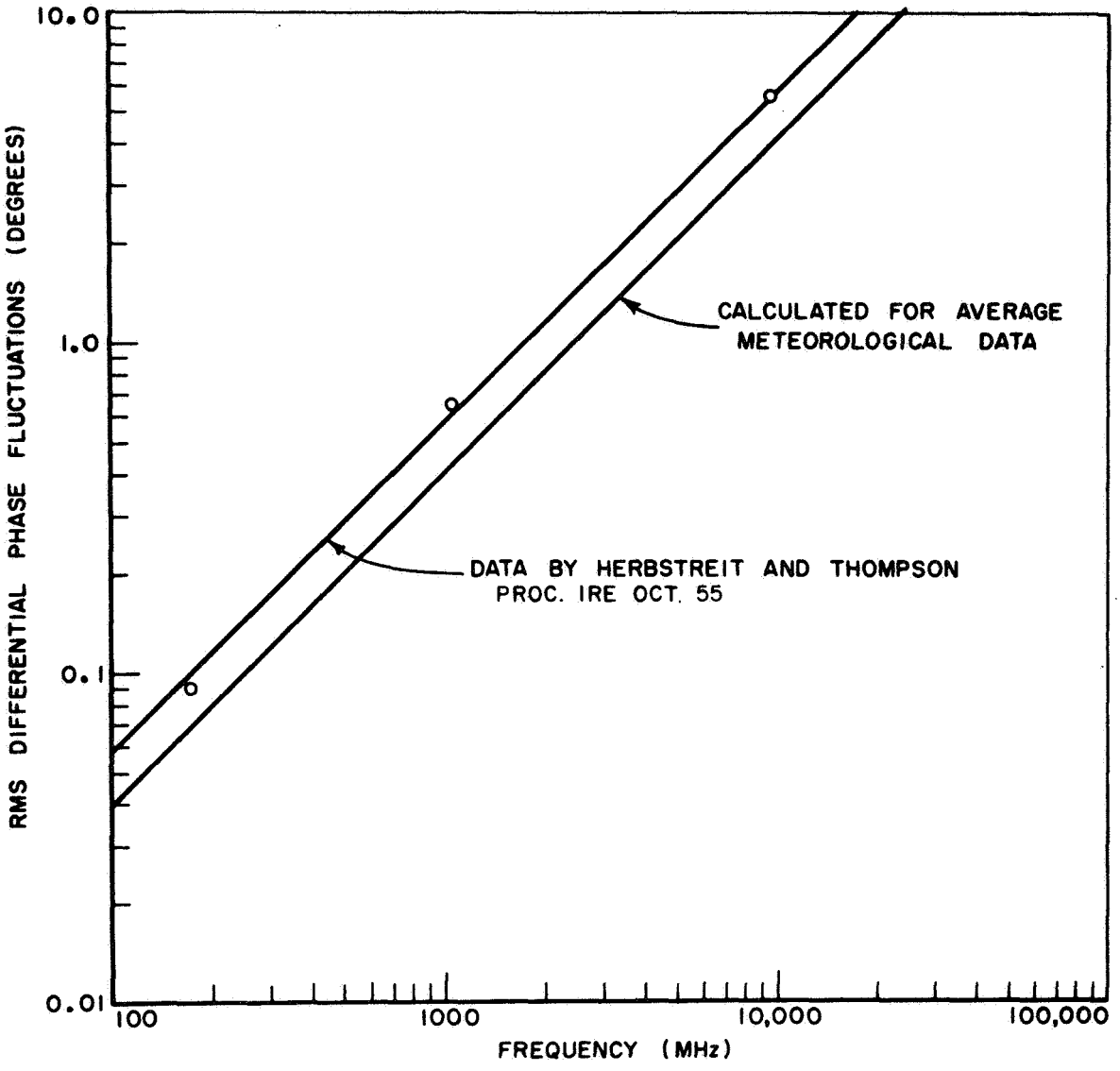

Fig. 2. Phase fluctuation vs. frequency.

A. Relative phase shift between two points

Frequently when studying large antenna apertures or arrays of antennas it is more desirable to consider the relative or differential phase shift between two points in the receiver plane. The geometry of this situation is shown in Fig. 3.

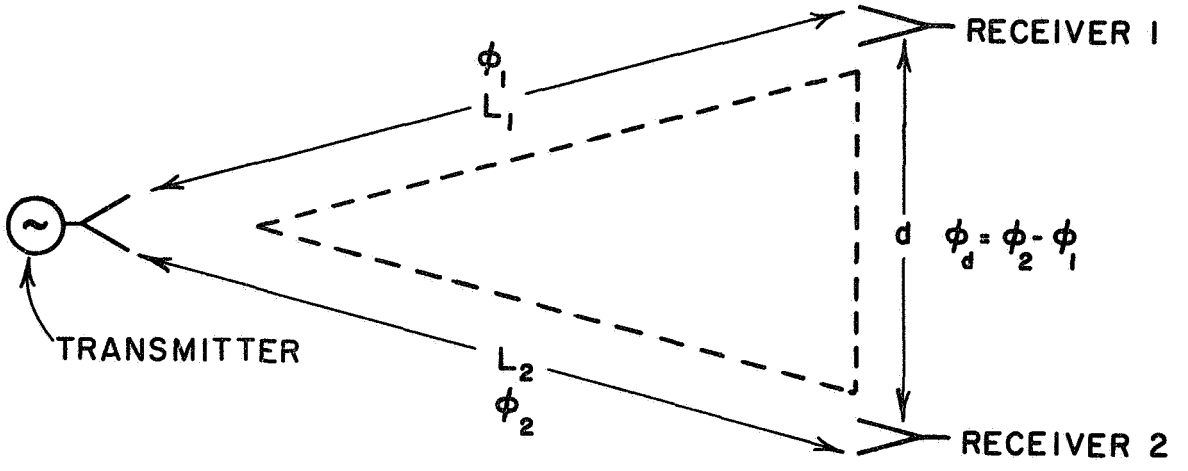

Fig. 3. Differential phase geometry.

The mean differential phase fluctuations between the two receivers is given by

$$\overline{\phi_d} = \overline{\phi_2 - \phi_1}$$

Again $\overline{\phi_d} = 0$ since $\overline{\Delta\eta} = 0$ so only the mean squared or root mean squared values are of importance.

$$(1) \qquad \overline{\phi_d^2} = \overline{(\phi_2 - \phi_1)^2} = \overline{\phi_2} - \overline{2\phi_1\phi_2} + \overline{\phi_1^2}$$

where for equal path lengths and isotropic turbulence $\overline{\phi_1^2} = \overline{\phi_2^2} = \overline{\phi^2}$. The cross product term in Eq. (1) can be rewritten in terms of a spatial correlation function ρ_{12} such that

$$\overline{\phi_1\phi_2} = \rho_{12}\overline{\phi^2}$$

so that $\overline{\phi_d^2} = 2\overline{\phi^2}\,(1-\rho_{12})$

or $\phi_{d(RMS)} = \sqrt{2}\ \phi_{RMS} \sqrt{1 - \rho_{12}}$.

As the two receivers become coincident ($\rho_{12} = 1$) the differential phase shift in zero. When the two receivers are widely seperated $d \rightarrow \infty$, $\rho_{12} \rightarrow 0$ the differential phase approaches it's maximum value $\sqrt{2\ \overline{\phi^2}}$.

For the particular frequency of interest, 16 GHz, the absolute phase fluctuations along the propagation path and maximum possible differential phase fluctuations between receivers are calculated as a function of path length (see Fig. 4); again the calculation is based on average troposphere conditions. The general relationship between phase fluctuations and separation distance is controlled as the factor $\sqrt{1-\rho_{12}}$ and is experimentally verified by the X band measurements[3] of Fig. 5.

B. The spatial phase correlation coefficient

The mathematical expression for the spatial phase correlation has been derived [4] for the two geometrical situations shown in Fig. 6. The common end point model is appropriate when the receiver is not a large distance from the transmitter. The parallel ray model applies to the case where the receiver is extremely far from the transmitter for example, a satellite-Earth link. The results are summarized in Table II.

TABLE II

Atmospheric Model for $C_{\eta\eta}$	ρ_{12} - Common End Point	ρ_{12} - Parallel Rays
Exponential	$\frac{\pi}{2}\left[K_o\left(\frac{d}{\ell_o}\right) L_{-1}\left(\frac{d}{\ell_o}\right) + L_o\left(\frac{d}{\ell_o}\right) K_{-1}\left(\frac{d}{\ell_o}\right)\right] - K_o\ \frac{d}{\ell_o}$	$\frac{d}{\ell_o}\ K_1\left(\frac{d}{\ell_o}\right)$
Gaussian	$\frac{\sqrt{\pi}}{2}\ \frac{\ell_o}{d}\ \mathrm{Erf}\left(\frac{d}{\ell_o}\right)$	$\epsilon^{-\frac{d^2}{\ell_o^2}}$
Cauchy	$\left[1 + \left(\frac{d}{\ell_o}\right)^2\right]^{-1/2}$	$\left[1 + \left(\frac{d}{\ell_o}\right)^2\right]^{-3/2}$

where K denotes Bessel function
L denotes Struve function
Erf denotes error function.

The spatial phase correlation coefficient for each of the models is nearly the same. For illustration Fig. 7 shows ρ_{12} for the common

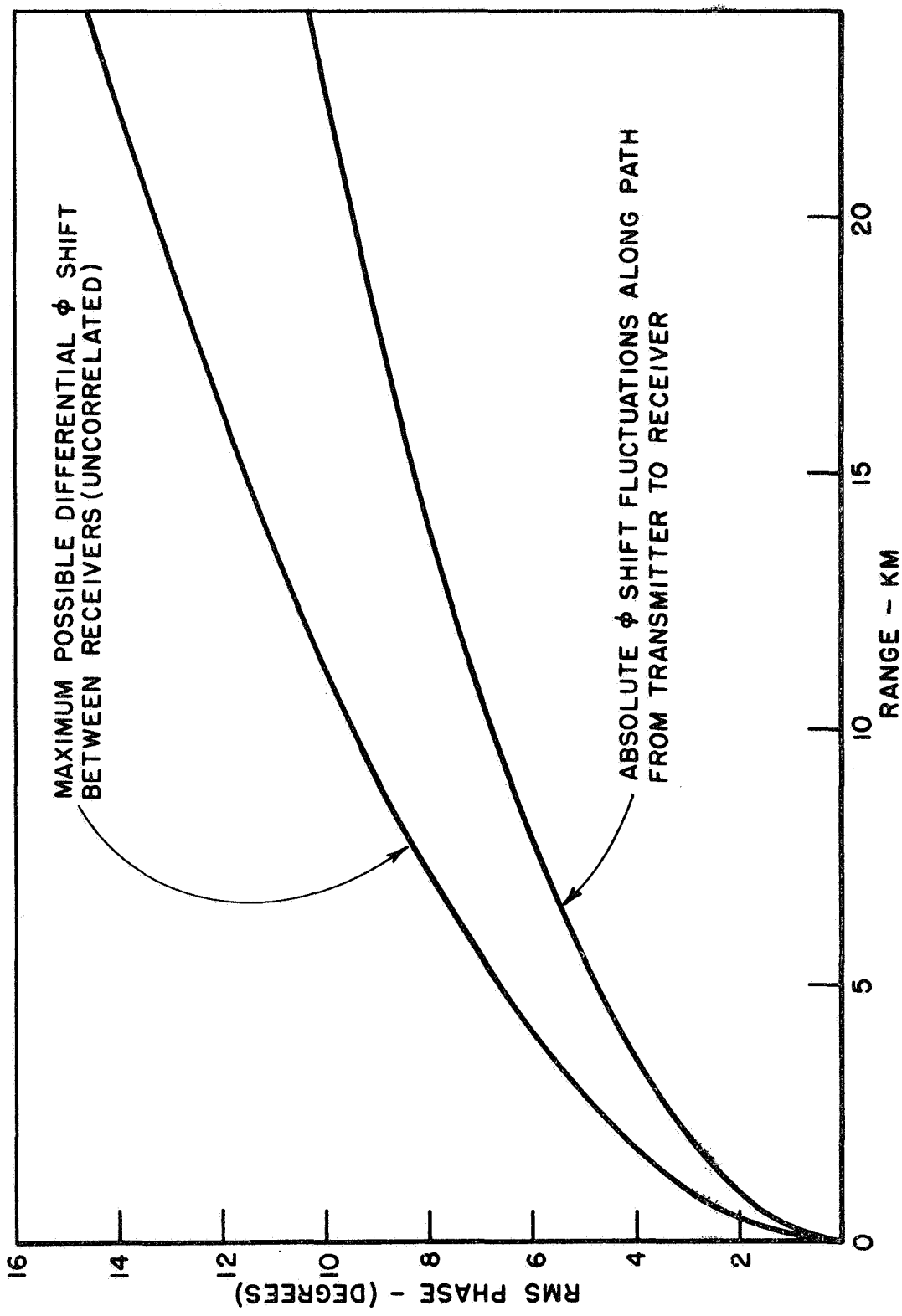

Fig. 4. 16 GHz phase fluctuations.

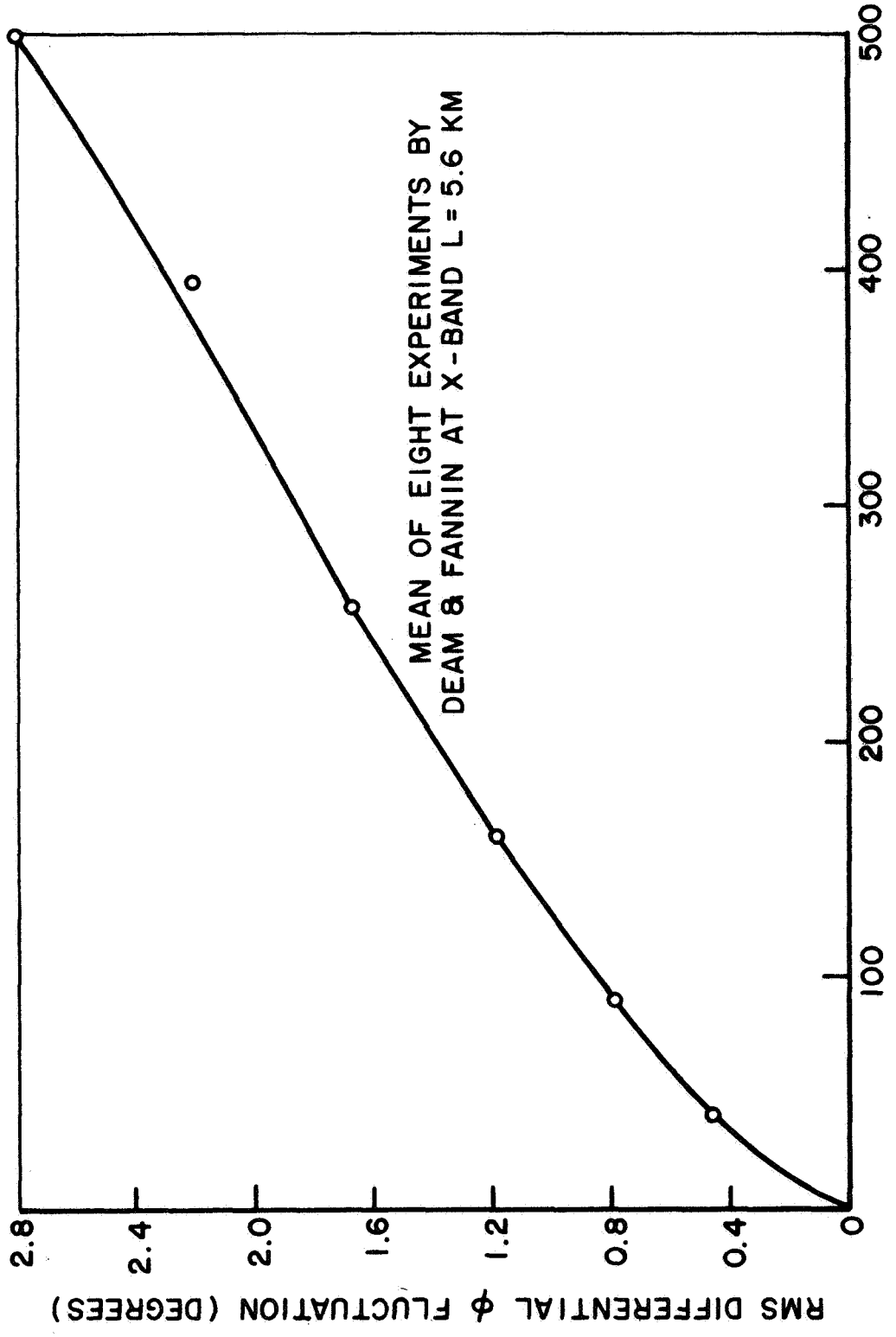

Fig. 5. Typical spatial phase correlation.

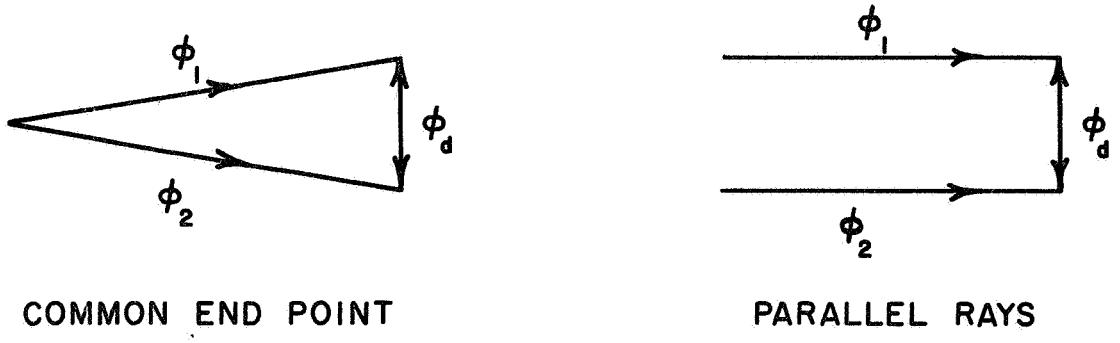

Fig. 6. Geometry of spatial phase correlation.

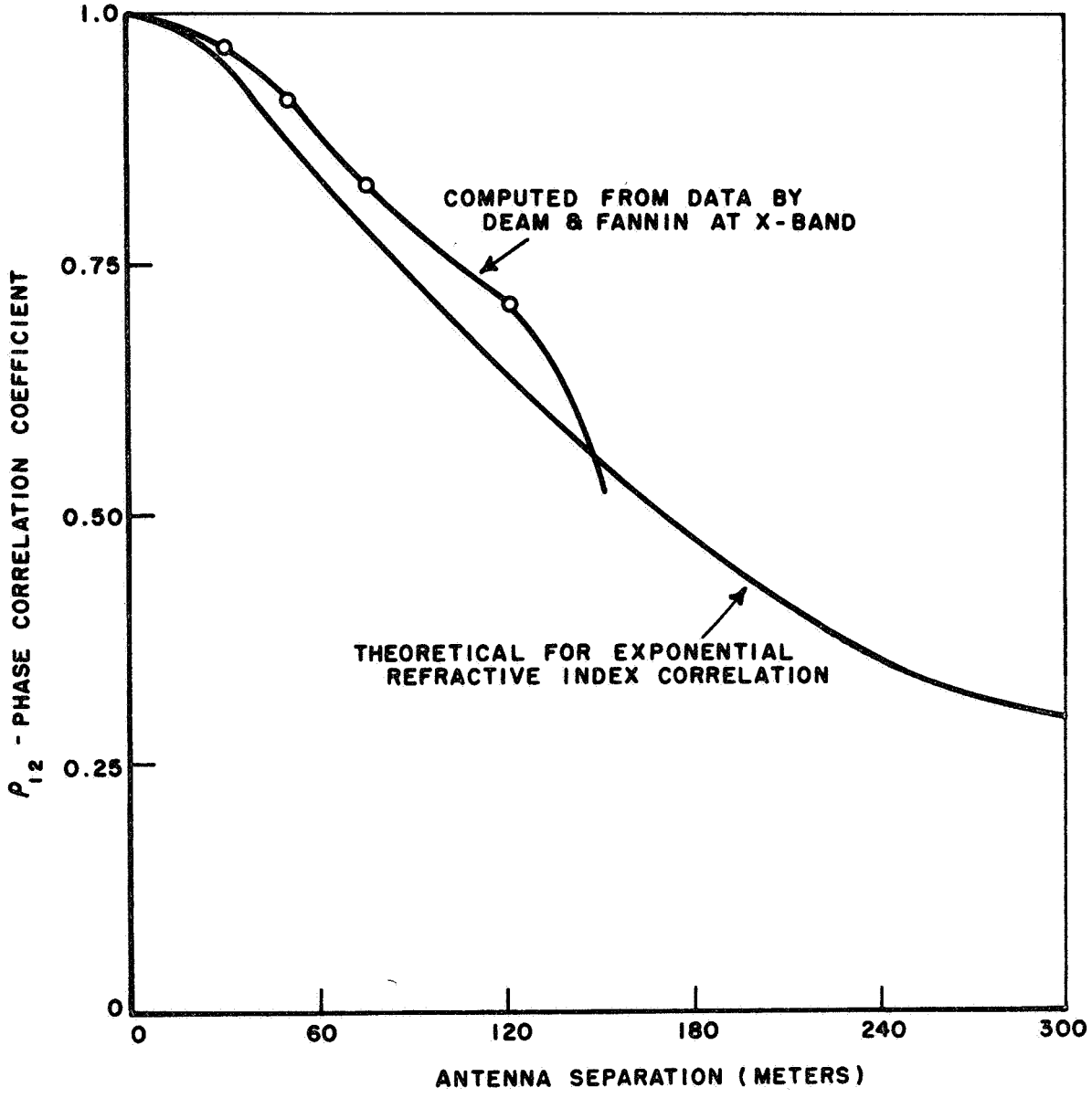

Fig. 7. Phase correlation coefficient.

end point, exponential refractive index model; for experimental verification ρ_{12} is also computed for X band measurements by Deam and Fannin.[3]

III. AMPLITUDE FLUCTUATIONS

There are two types of amplitude variations to be considered, a randomly fluctuating component present even under normal atmospheric conditions, and a component due to changes in the meteorological status such as rain, snow, fog, etc.

A. Normal Atmospheric Condition

It is well known that the non homogeneities of the propagation medium cause scattering of the incident field, which in turn produces a fluctuation in the amplitude at the receiver plane.

Several models have been proposed to relate these amplitude fluctuations to phase fluctuations. One model assumes the received field to be composed of a direct component plus a phase-quadrature, normally distributed component. On the basis of this model the following relationship is derived.[5]

$$\sigma_\phi^2 \approx 2\ \sigma_a$$

where σ_ϕ^2 = variance of phase fluctuations

σ_a = square root of variance of amplitude fluctuations divided by the mean amplitude.

Another model assumes the received field to be the vector sum of a constant component plus a small Rayleigh scattered component arriving from off axis non homogeneities in the propagation medium. For this model the corresponding relationship is given by[6]

$$\sigma_\phi^2 \approx \sigma_a^2 .$$

Measurements obtained by Herbstreit and Thompson[7] generally fall between those predicted by the two models.

The results of some experimental data on amplitude scintillations are tabulated in Table III. It can be seen that the component of random amplitude fluctuation during normal tropo conditions is in general quite small.

TABLE III

Typical Experimental Measurements of
Amplitude Fluctuations

Experimenter	Organization	Frequency	Path Length	Reported Results	Reference
Deam & Fannin	University of Texas	9.4 GHz	5.6 Km	less than $\pm$.2 dB about mean	3
Waterman & Lee	Stanford	35 GHz	28 Km	1 dB peak-peak	16
Sukhia	Martin-Orlando	16 GHz 35 GHz	5.6 Km 12.5 Km	less than 1 dB about 1 dB	17
Etcheverry et al.	Aerospace Corporation	93 GHz	19 Km	3 dB peak-peak for clear, 2-5 knot winds	18

These amplitude scintillations are superposed upon the attenuation losses in the path due to oxygen and water vapor absorption. The percentage of O_2 in the atmosphere remains almost constant as a function of time but the H_2O vapor content may have a seasonal variational of 20:1;[8] hence the attenuation loss is not a constant, but if the pressure, temperature, and H_2O content are known the attenuation per unit length can be computed using the formulas derived by Van Vleck.[9]

Representative values of measured absorption losses due to O_2 and H_2O for the frequency range 10 - 200 GHz are shown in Fig. 8.[10] Figure 9 summarizes the attenuation through the entire atmosphere as a function of elevation angle.[11]

B. Abnormal Atmospheric Condition

In addition to the rapid fluctuations (a few cps) in amplitude and the slowly varying change in attenuation due to H_2O vapor, abnormal conditions such as rain, snow, and fog may considerably change the amplitude of the received signal.

Figure 10 shows the attenuation due to rainfall for several rates.[12] It can be seen that additional losses in the order of 10 dB/Km are possible in the mm region.

Considerable research has been done by Bell Telephone Laboratories[13] on obtaining the statistical data for both the temporal and spatial distribution of rainfall using one hundred electronic rainfall gauges over an area of 130 square kilometers. Initial measurements indicate that heavy rainfall rates occur over a relatively small area at any given time so that spatial diversity techniques could be used to considerably increase communication reliability during severe rainstorms.

IV. FREQUENCY CROSS CORRELATION

A. Amplitude and Phase Considerations

Bandwidth limitations by the propagation medium for line of site paths is a problem of considerable current interest. Indeed wide bandwidth with its corresponding high data rate potential is one of the most important factors which make the microwave-mm region appealing.

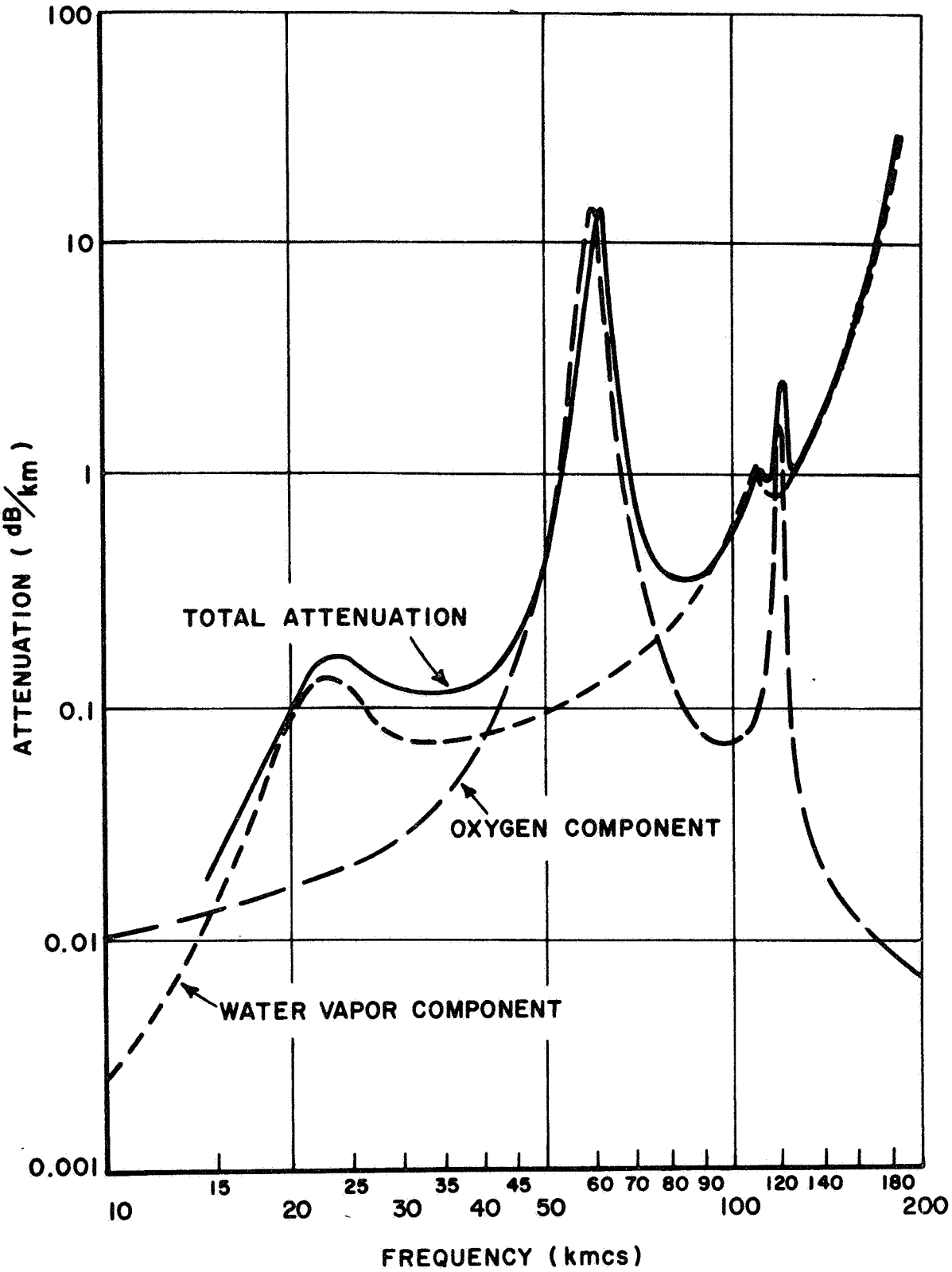

Fig. 8. Attenuation vs. frequency.

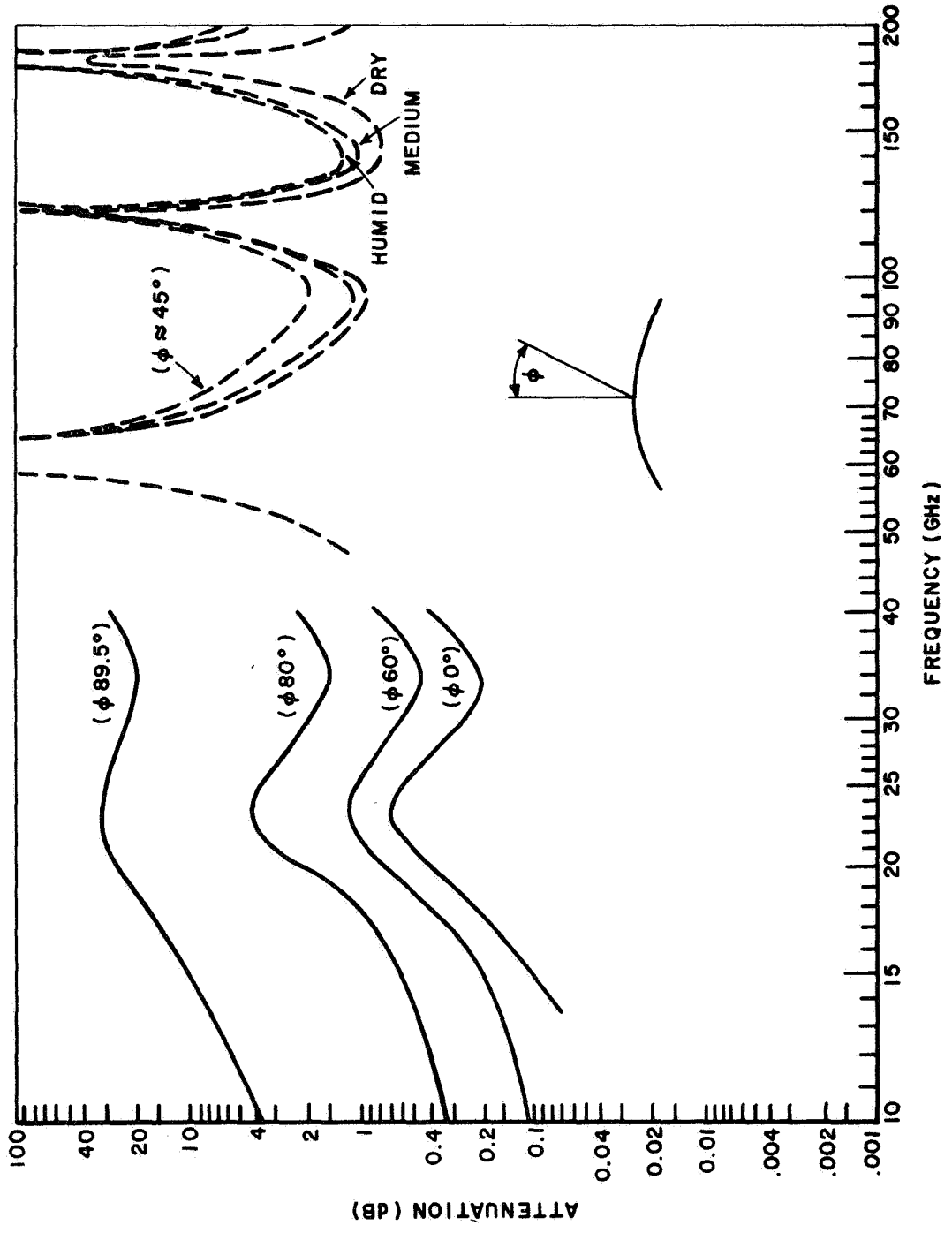

Fig. 9. Attenuation thru the entire atmosphere.

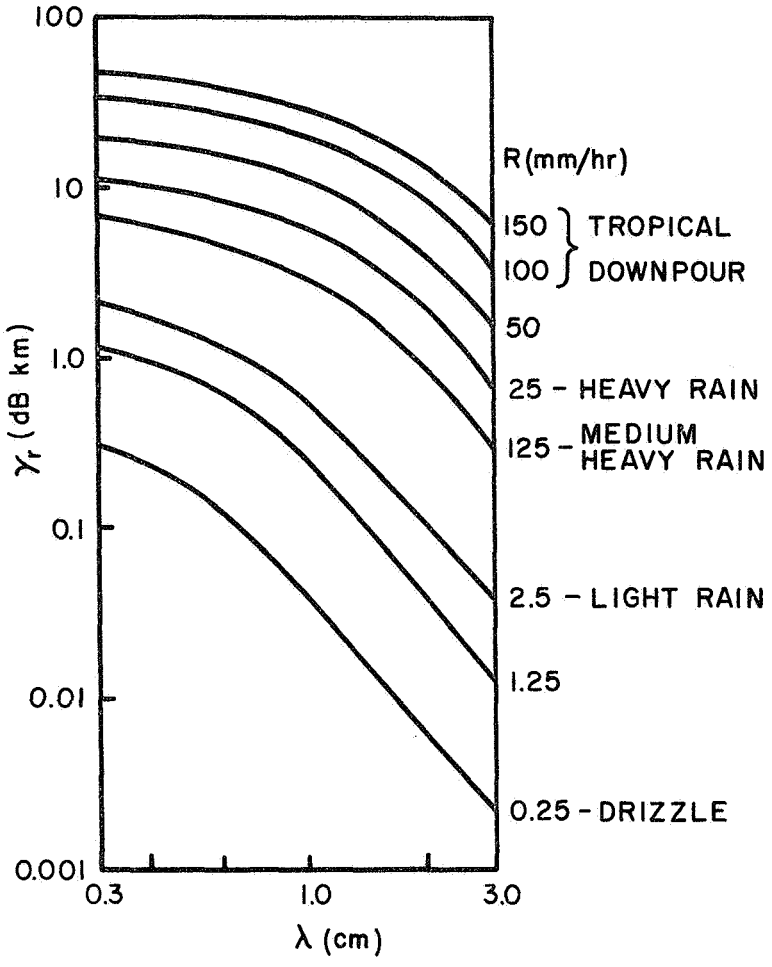

Fig. 10. Attenuation for various rain rates.

To understand the physical mechanism of this problem consider Fig. 11. If the medium were uniform and non turbulent only the direct line-of-site component would be received at the point of observation. If, however, turbulence exists and small scattering inhomogeneities are present then a small amount of energy will be refracted by the off axis scattering bodies into the receiver. The total received voltage v_r can be expressed as a sum of the direct line-of-site component v_α plus the scattered component v_s as shown in Fig. 12. For convenience the resultant scattered field may be resolved into two quadrature components which are in phase (v_{sy}) and orthogonal (v_{sx}) to the direct component.[14]

The total received voltage has a mean value given by

$$\overline{v_r} = \sqrt{\overline{v_{sx}^2} + (v_\alpha + v_{sy})^2}$$

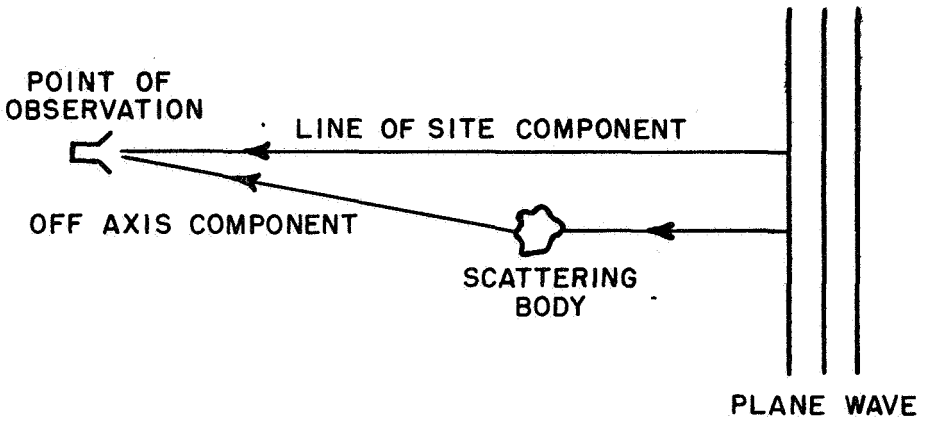

Fig. 11. Off axis scattering.

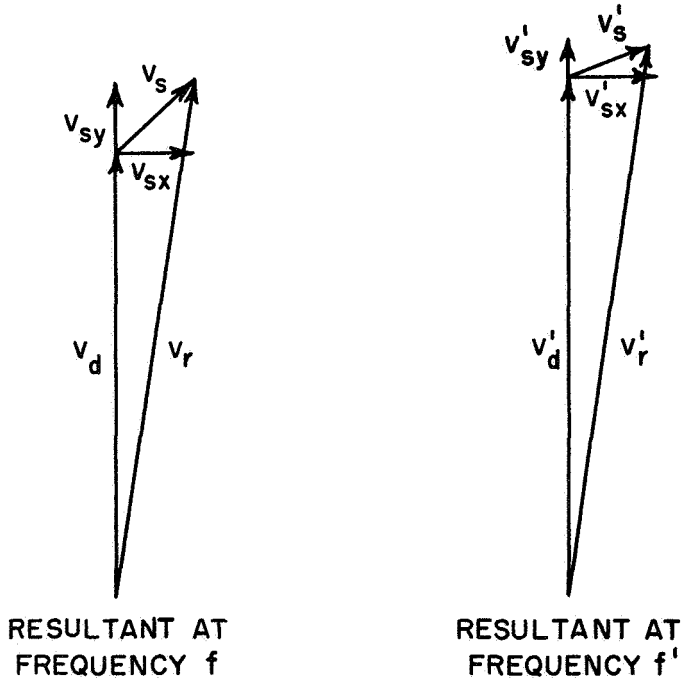

Fig. 12. Vector sum of components at frequency f and f'.

where the overbar again denotes ensemble average; v_r fluctuates about its mean value by Δv_r, i.e.

$$v_r = \overline{v_r} + \Delta v_r$$

or

$$\Delta v_r = \sqrt{\overline{v_{sx}^2 + (v_d + v_{sy})^2}} - \sqrt{\overline{v_{sx}^2 + (v_d + v_{sy})^2}} \tag{2}$$

Similarly the phase fluctuations are given by

$$\Delta\phi = \arctan\left(\frac{v_{sx}}{v_d + v_{sy}}\right) \tag{3}$$

In order to determine the scintillation coherence properties between adjacent frequencies f and $f = f + \delta f$ it is again convenient to introduce an amplitude and phase frequency cross correlation coefficient given by

$$C_a(\delta) = \frac{\overline{\Delta v_r \, \Delta v'_r}}{\Delta v_{r_{RMS}} \Delta v'_{r_{RMS}}} \qquad \text{for amplitude}$$

and

$$C_\phi(\delta) = \frac{\overline{\Delta\phi \, \Delta\phi'}}{\Delta\phi_{RMS} \Delta\phi'_{RMS}} \qquad \text{for phase}$$

For the case where the fluctuation in amplitude and phase are small compared to their mean value, these correlation functions can be expanded using Eqs. (2) and (3). Keeping only quadratic terms yields

$$C_a(\delta) = \frac{\overline{v_{sy} \, v'_{sy}}}{\sqrt{\overline{v_{sy}^2} \; \overline{v'^2_{sy}}}}$$

$$C_\phi(\delta) = \frac{\overline{v_{sx} \, v'_{sx}}}{\sqrt{\overline{v_{sx}^2} \; \overline{v'^2_{sx}}}}$$

It is now only necessary to obtain the expressions for the fluctuating components v_{sx} and v_{sy}, which can be derived from a perturbation solution of the wave equation using the Born approximation (single scattering).

For the Gaussian model of atmosphere refractive index correlation the following expressions have been derived.

$$\overline{v_y v'_y} = \frac{E_o^2 \pi^{5/2} \overline{\Delta\epsilon^2} L\ell_o (1+\delta)}{4\lambda^2} \left[-M\left(\frac{1}{b\eta_1}\right) + M\left(\frac{1}{c\eta_1}\right) \right]$$

$$\overline{v_x v'_x} = \frac{E_o^2 \pi^{5/2} \overline{\Delta\epsilon^2} L\ell_o (1+\delta)}{4\lambda^2} \left[-M\left(\frac{1}{b\eta_1}\right) - M\left(\frac{1}{c\eta_1}\right) \right]$$

where

$$M(x) = x \sin x \, Ci(x) + x \cos x \, Si(x)$$

$$Ci(x) = \int_x^\infty \frac{\cos u}{u} \, du$$

$$Si(x) = -\int_x^\infty \frac{\sin u}{u} \, du$$

$$\eta_1 = \frac{L\lambda}{2\pi \ell_o^2}$$

$$b = \frac{\delta}{1+\delta}$$

$$C = \frac{2+\delta}{1+\delta}$$

B. Results and Experiments

For convenience the numerical solution for the amplitude and phase frequency cross correlation coefficient is shown in Fig. 13. It can be seen that in general both amplitude and phase fluctuations are well correlated over extremely wide frequency bands. Amplitude correlation of 0.4 to 0.9 over a 1.5 to 1 frequency spread has been reported by Burrows and Little.[15] Phase correlation of 0.7 to 0.9 over a 10 to 1 frequency spread (f = 1 GHz, f' = 10 GHz) has been reported by Deam and Fannin.[3]

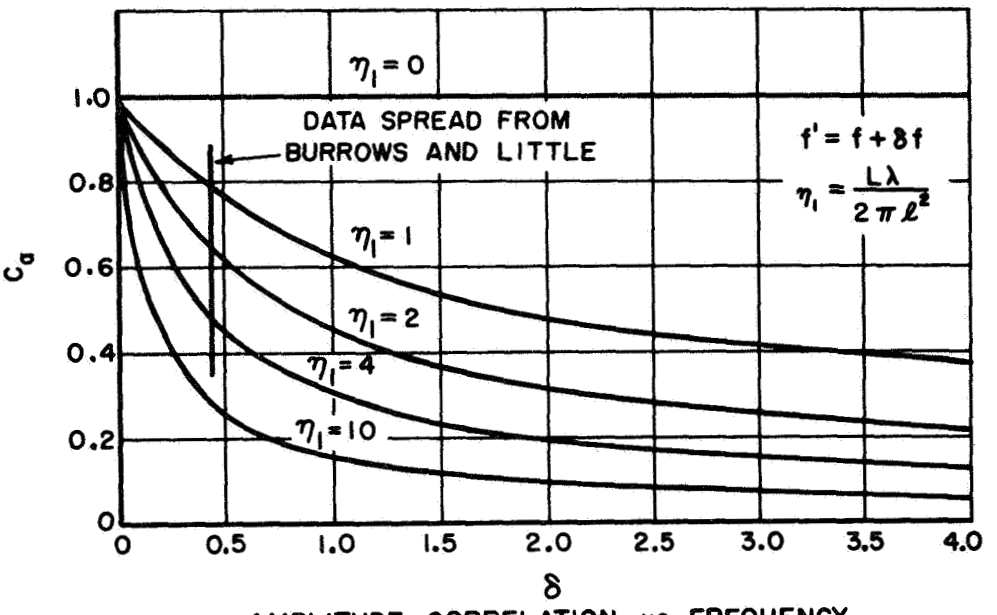

AMPLITUDE CORRELATION vs FREQUENCY

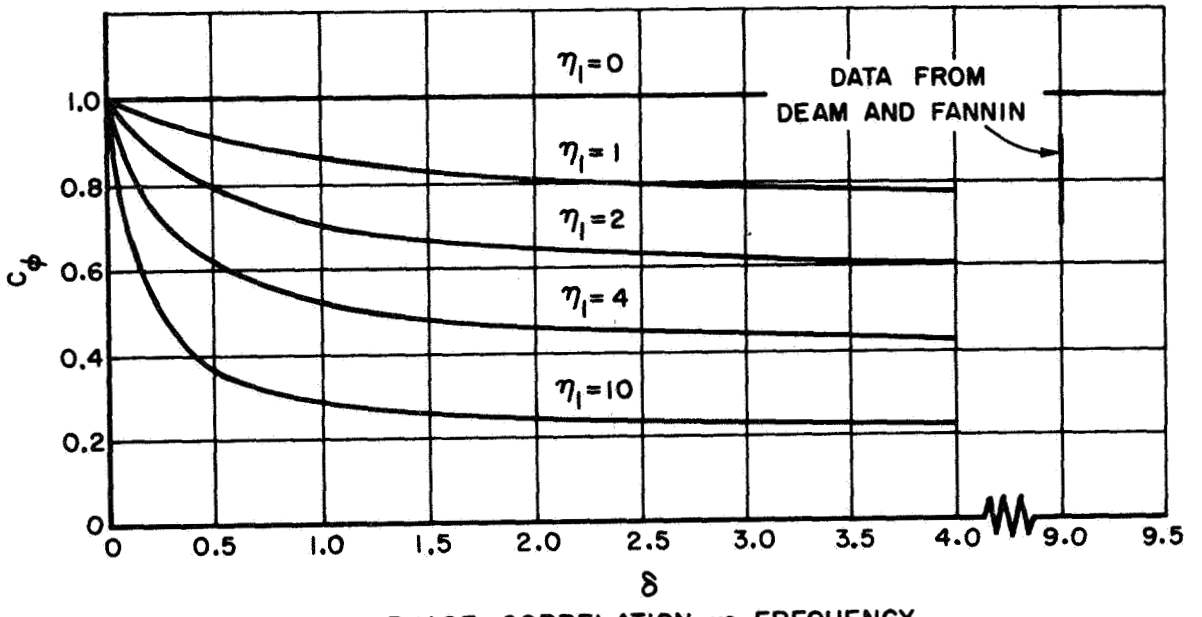

PHASE CORRELATION vs FREQUENCY

Fig. 13. Amplitude and phase correlation vs. frequency difference.

1. Oliver, T. L., "Atmospheric Attenuation and Sky Noise Temperature in the Microwave and Millimeter Wave Spectrum," Report 2440-2, 1 May 1968, ElectroScience Laboratory, Department of Electrical Engineering, The Ohio State University; prepared under Contract F33615-67-C-1663 for Air Force Avionics Laboratory, Wright-Patterson Air Force Base, Ohio.

2. Muchmore, R. B. and Wheelon, A. D., "Line-of-Site Propagation Phenomena-I. Ray Treatment" Proc. IRE, October 1955.

3. Deam, A. and Fannin, B., "Phase Difference Variations in 9350 MHz Radio Signals Arriving at Spaced Antennas," Proc. IRE, October 1955.

4. Muchmore, R. B. and Wheelon, A. D., op cit.

5. Norton, K. A., et al., "Probability Distribution of Amplitude of a Constant Vector Plus a Rayleigh Distributed Vector," Proc. IRE, October 1955, pp. 1354.

6. Norton, K. A., et al., "The Probability Distribution of the Phase of the Resultant Vector Sum of a Constant Vector Plus a Rayleigh Distributed Vector," Journal of Applied Physics, Vol. 23, January 1952, pp. 137.

7. Herbstreit and Thompson, "Measurement of the Phase of Radio Waves Received over Transmission Paths with Electrical Length Varying as a Result of Turbulence," Proc. IRE, October 1955.

8. Wulfsberg, K. N., "Apparent Sky Temperature at mm-Wave Frequencies," Physical Science Research Paper #38, July 1964, Air Force Cambridge Research Laboratories.

9. Van Vleck, J. H., "Propagation of Short Radio Waves," MIT Radiation Lab Series.

10. Tolbert, et al., "Radio Propagation Measurements in the 100-118 GHz Spectrum," EERL University of Texas Report #107.

11. Rosenblum, E. S., "Atmospheric Absorption of 10-400 GHz Radiation: Summary and Bibliography to 1960," MIT Lincoln Lab Report 82-G-0021, ASTIA #242598, August 1960.

12. Wirbel and Dressle, "Propagation Studies in Millimeter-Wave Link Systems," April 1967 Proc. IEEE, pp. 497.

13. Semplak, R. A., "A Dense Rain Gauge Measuring System for Attenutation Studies of Radio Propagation," Paper given at Spring 1967 URSI Meeting, Ottawa, Canada.

14. Muchmore and Wheelon, "Frequency Correlation for Line-of-Site Signal Scintillations," PGAP, January 1963, pp. 50.

15. Burrows and Little, "Simultaneous Observations of Radio Star Scintillations on Two Widely Spaced Frequencies," Jodrell Bank Annals, Vol. I, 1952.

16. Waterman and Lee, "A Large Antenna Antenna Array for mm Wave Propagation Studies," Proc. IEEE, April 1966.

17. Sukhia, Don, telephone conversation, 16 February 1967.

18. Etcheverry, et al., "Measurements of Spatial Coherence in 3.2 mm Horizontal Transmission," IEEE-PGAP, January 1967.